Verification of macro-element method for vertical drains in dynamic problem

Vérification de méthode de macro-élément pour les canalisations dans le problème dynamique

Toshihiro Nonaka
Disaster Mitigation Research Center, Nagoya University, Japan, nonaka@nagoya-u.jp

Shotaro Yamada
Department of Civil Engineering, Nagoya University, Japan

ABSTRACT: In the simulation of the vertical drain method using a soil-water couple finite element analysis, macro-element method can be used as an approximate method to introduce the water absorption and discharge functions of drains into individual elements. Although in most cases this method had been applied to quasi-static problems, the authors extend the function of the method and applied it to the soil-water coupled analysis code ***GEOASIA*** with an inertial term to evaluate the countermeasure effect of the pore water pressure dissipation method against liquefaction. In this paper, in order to verify the new macro-element method in dynamic problem under plane strain condition, the results of 2D analysis using the new macro-element method was compared with those of 3D analysis in which vertical drains were represented exactly by finely dividing finite element meshes. This paper presented that 2D analysis using the new macro-element method can approximate 3D analysis with fine mesh accurately in dynamic problem in terms of excess pore water pressure change and ground deformation.

RÉSUMÉ: Dans la simulation d'une méthode de drainage utilisant une analyse d'éléments finis couplée sol-eau, la méthode macro-élément peut être utilisée comme une méthode approximative pour introduire l'absorption hydraulique et déverser les fonctions de drainage dans les éléments individuels. Bien que cette méthode ait été appliquée seulement à des problèmes quasi-statiques, l'auteur étend la fonction de la méthode et l'applique à l'analyse couplée sol-eau code ***GEOASIA*** avec un terme interstitiel pour évaluer l'effet de contre-mesure de la méthode de dissipation de la pression hydraulique interstitielle par rapport à la liquéfaction. Dans cet article, afin de vérifier la nouvelle méthode macro-élément en problème dynamique dans des conditions de déformation plane, les résultats de l'analyse bi-dimensionnelle utilisant la nouvelle méthode macro-élément ont été comparés avec ceux de l'analyse tri-dimensionnelle dans laquelle les drainages verticaux ont été exactement représentés en divisant finement les mailles des éléments finis. Il est montré que l'analyse bi-dimensionnelle utilisant la nouvelle méthode de macro-éléments peut s'approcher de l'analyse tri-dimensionnelle avec une maille fine en problème dynamique précisément en termes de changement de pression hydraulique interstitielle excédentaire et de déformation du sol.

KEYWORDS: Pore water pressure dissipation method; Soil-water coupled analysis; Macro-element method

1 INTRODUCTION

One of the issues with numerical analysis of the pore water pressure dissipation Method (hereinafter referred to as PWPDM) is the enormous calculation cost because three-dimensional (3D) analysis with fine mesh is required to represent a large number of vertical drains installed in ground. The authors (Yamada et al. 2015) have focused on the macro-element method, proposed by Sekiguchi et al. (1986), as a means to resolve this issue. Since the macro-element method introduces the water absorption and discharge functions of drains into individual elements under two-dimensional (2D) plane strain condition without using fine mesh, it is possible to improve calculation efficiency dramatically. Although in most cases this method had been applied to quasi-static problems, the authors applied it to dynamic problem by equipping it with the soil-water coupled analysis code ***GEOASIA*** (Noda et al. 2008) with an inertial term (Noda et al. 2015). In PWPDM, liquefaction during earthquake is inhibited by suppressing the increase in pore water pressure by means of the installation of vertical drains. Instead of this, some degree of ground surface settlement due to compaction must be allowed for. Accordingly, in addition to the question of whether or not the method can be used to prevent liquefaction, it is important to be able to predict the degree of deformation that will occur as a result of ground compaction. This is another issue with numerical analysis of PWPDM. ***GEOASIA*** is capable of handling the following phenomena uniformly: 1) both compaction and liquefaction and 2) both the settlement due to compaction during earthquake and the consolidation settlement after liquefaction. Therefore, it can also overcome this issue at the same time.

In this paper, in order to verify the new macro-element method in dynamic problem under plane strain condition, the results of 2D analysis using the new macro-element method was compared with those of 3D analysis in which vertical drains were represented exactly by finely dividing finite element meshes, taking a case of sand ground improved by PWPDM under the embankment as an example.

2 ANALYSIS CONDITIONS

As shown in Fig. 1, a case of sand ground improved by PWPDM under an embankment was assumed as an analysis target. Grid drains with rectangular cross section (Research Association for DEPP Method 2011) (width 150 mm, thickness 50 mm) with a constant drain spacing in square pattern were installed in the soft sandy layer beneath the embankment. A drainage mat was spread between ground and embankment in order to avoid blocking drainage from drains.

Figure 2 shows the finite element mesh and the boundary conditions for the 3D mesh-based analysis in which vertical drains were represented exactly by finely dividing finite element meshes (hereinafter referred to as exact model). For simplicity, a single row of drains perpendicular to the embankment was targeted for the analysis. Furthermore, symmetry was assumed, so the region that enclosed by the dashed lines in the plan view in Fig. 1 was used actually for the analysis. The elements representing the drains themselves were assigned the same material properties as the surrounding soil.

And permeable boundary was assigned between the elements representing drains and the elements adjacent to them horizontally in order to represent the water absorption and discharge functions of drains. The drainage mats were assumed to be under atmospheric pressure. The side of the element representing the drain was subjected to hydrostatic pressures corresponding to the depth from the top of drain. In the exact model, it was necessary to use a fine mesh around the drains.

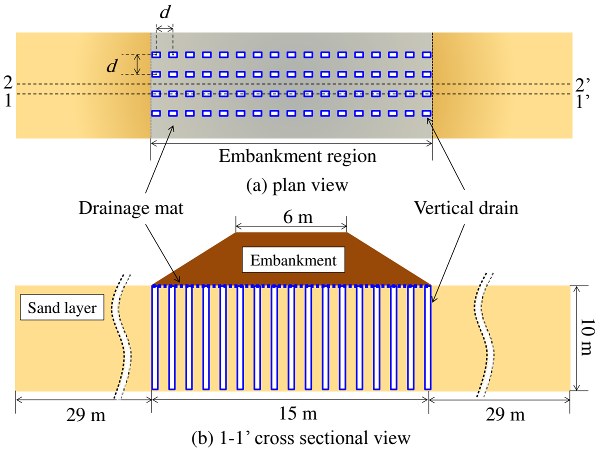

Figure 1. Outline figure of analytical model

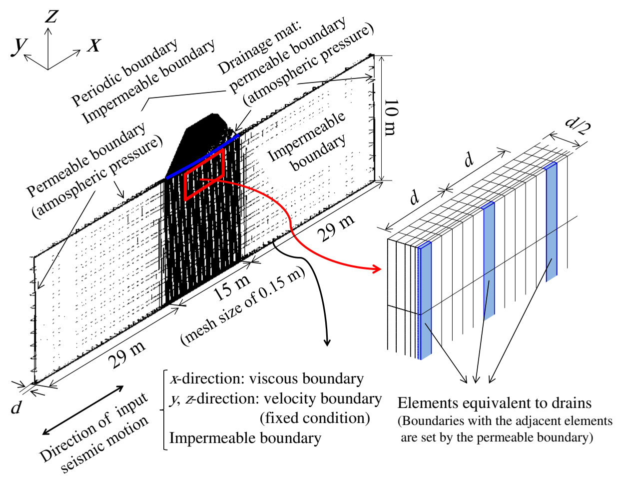

Figure 2. Finite mesh and boundary conditions (exact model)

Figure 3 presents the finite element mesh and the boundary conditions for the 2D mesh-based analysis using the macro-element method (hereinafter referred to as approximate model). Macro-element method was applied to the elements in the region enclosed by the dashed lines. As with ground, boundary conditions of macro-element were assumed to be atmospheric pressure at the top and assumed to be impermeable at the bottom. In macro-element method proposed by the authors (Yamada et al. 2015, Noda et al. 2015), the mesh division width can be separated from the drain arrangement and spacing, so it is possible to conduct calculations with differing drain spacing via a single type of mesh that is relatively coarse.

While the drains were represented with permeable boundary conditions in the exact model, the drains were modeled with finite permeability in the approximate model. The results of analysis using macro-element method indicated that water pressures in the drains nearly equaled the hydrostatic distributions, so difference in representation about the permeability of drain does not matter especially in this study.

Embankment elements of 3 m high were added atop the horizontally layered sand ground in both models and consolidation calculations were continued until the models reached steady state. These embankment-ground systems were subjected to the triple linked-type seismic motions shown in Fig. 6 (orange line) in the x direction through viscous boundary.

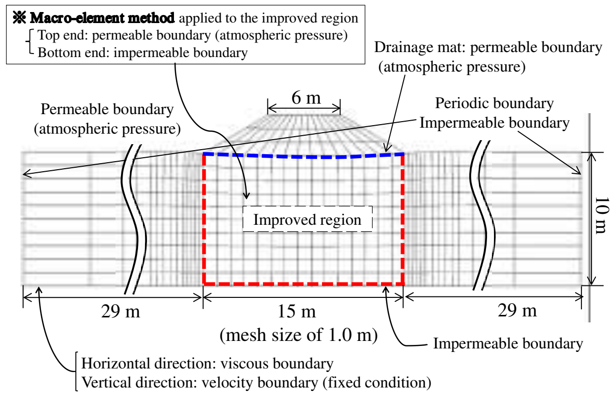

Figure 3. Finite mesh and boundary conditions (approximate model)

Table 1. Material constants and initial values (Noda et al, 2015)

	Sand	Embankment
Elasto-plastic parameters		
Critical state index M	1.00	1.35
NCL intercept N	1.98	1.71
Compression index $\tilde{\lambda}$	0.050	0.110
Swelling index $\tilde{\kappa}$	0.016	0.020
Poisson's ratio ν	0.3	0.3
Evolution parameters		
Degradation index of structure a	2.20	2.00
Degradation index of OC m	0.10	0.50
Rotational hardening index b_r	3.50	0.10
Limitation of rotational hardening m_b	0.70	0.40
Fundamental parameters		
Soil particle density ρ_s (g/cm^3)	2.65	2.67
Permeability index k (cm/s)	1.0×10^{-3}	1.0×10^{-4}
Initial conditions		
Specific volume v_0	0.8	0.8
Stress ratio η_0	4.0	1.1
Degree of structure $1/R^*_0$	1.2	42.5
Degree of anisotropy ζ_0	0.0	0.0

Table 2. Material constants of viscous boundary

Bedrock density ρ (g/cm^3)	2.0
S-wave velocity in bedrock V_s (m/s)	570.0

Table 3. Material constants of macro-element method

Drain spacing d (m)	0.9	0.6
Equivalent diameter d_e (m)	1.02	0.68
Diameter of circular drain d_w (m)	0.10	0.10
Permeability of circular drain k_w (cm/s)	7.0x10^2	7.0x10^2

Table 1 shows the material constants and initial values for the ground and embankment, and Table 2 shows the material constants for the viscous boundary. The ground was the same as in a previous study (Noda et al. 2015), and it was assumed to be a loose sandy soil. Table 3 provides the material constants for the drains, i.e., macro-element. Equivalent diameter d_e and drain diameter d_w were specified so that the areas of circles were equivalent to the improved area of a drain and the cross-sectional area of a drain. Three cases were examined, unimproved, drain spacing d were 0.9 m and 0.6 m, and the results of the exact model and those of approximate model were compared. In order to gain a direct grasp of only the improvement provided by the drains, the boundary between ground and embankment was assumed to be atmospheric pressure also in the unimproved cases.

3 ANALYSIS RESULTS

Figure 4 shows the distribution of excess pore water pressure (hereinafter referred to as EPWP) after the end of seismic motions (145 sec). Aside from the unimproved case, the exact model shows distributions along three distinct vertical (x-z) planes. In the unimproved case, the pore water pressure is high below the embankment. In both improved cases, however, the increase in water pressure below the embankment is suppressed by the discharge function of drains. In addition, the case with the smaller drain spacing has a greater effect of suppression of increase in water pressure. The exact model indicates great effect of suppression in the vicinity of the drains, even though this diminishes with distance from the drains. The distribution of EPWP of the approximate model in the case of d = 0.9 m shows the value that is near to the distribution at 0.3 m away from drains of the exact model, and that in the case of d = 0.6 m shows the value that is near to the distribution at 0.2 m away from drains of the exact model. As shown above, the approximate model is able to express differences in suppression of water pressure due to changes in drain spacing.

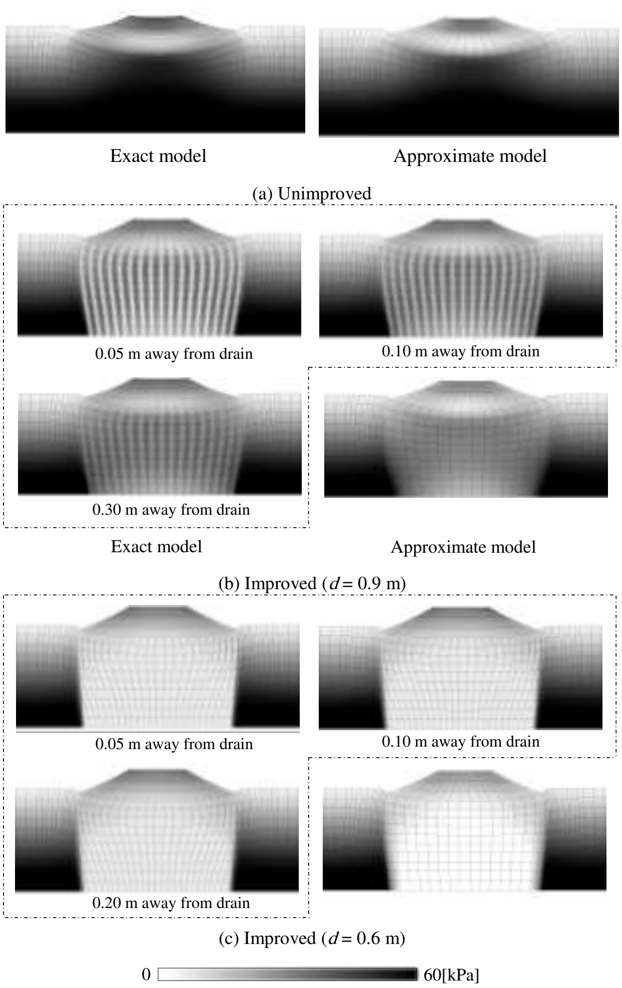

Figure 4. Distribution of EPWP (x-z cross section, 145seconds).

Figure 5 shows the relationship between time and EPWP ratio at the center of improved region. Results at the initial depths of 1.5, 4.5, and 7.5 m are shown. For the exact model, EPWP ratio is the average value weighted by the volume for horizontally adjacent elements in the improved region assigned to the center drain. The unimproved case shows a high EPWP ratio until the end of the seismic motion. In contrast, in the two improved cases, even though EPWP ratio increases until the input acceleration reaches its highest value, subsequent to that, EPWP ratio decreases with the passage of time due to the effect of drains. Additionally, the case with smaller drain spacing shows a sharp dissipation of water pressure. The approximate model evaluates the effect of drain spacing on suppression of increase in water pressure quantitatively in all depths.

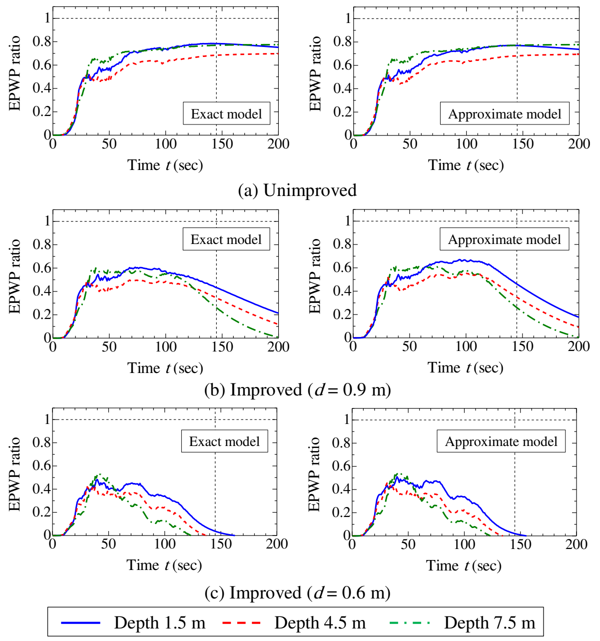

Figure 5. Time-EPWP ratio

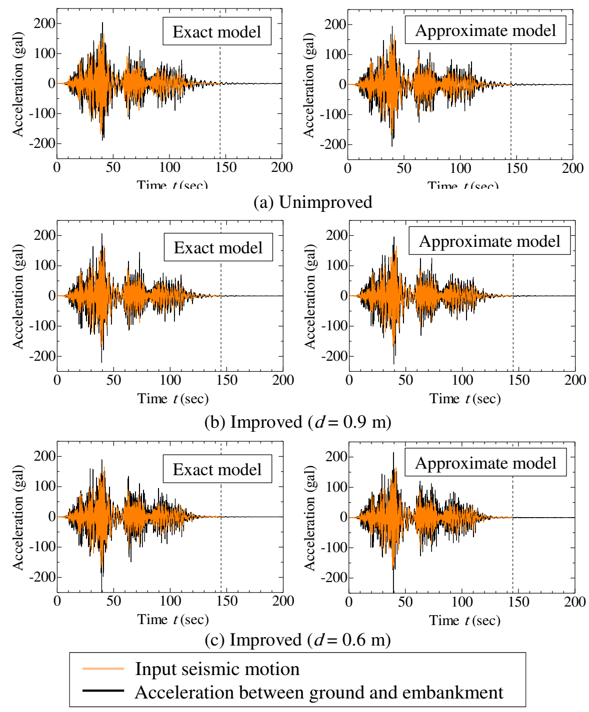

Figure 6. Acceleration response (x direction)

Figures 6 and 7 show the time-horizontal acceleration and the time-settlement relationships at the center of the boundary between ground and embankment, respectively. The results of the exact model are the values for the nodes in contact with drains. It was confirmed that nearly identical results were obtained at other nodes in the y direction. The approximate model provides responses equivalent to those of the exact model in all figures. The closer the drain spacing is, the greater the suppression of increase in water pressure is, and the better the stiffness of ground is preserved. Because of this, the amplification of acceleration and the reduction in settlement occurred. The results of the approximate model reproduce features as described above. The responses of the exact and approximate models are nearly identical for the unimproved case, thereby suggesting that the mesh size has little influence over results.

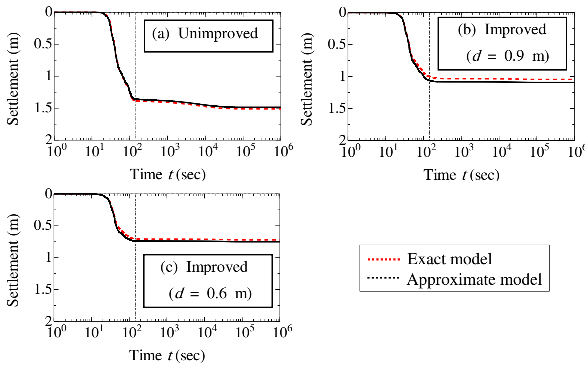

Figure 7. Settlement behavior

Figure 8 shows the deformation of the improved region and the embankment after consolidation. The horizontal displacement is relative to the center nodes of the bedrock (bottom of the analytical region). In the two improved cases, since the decrease of the effective stress is inhibited and the shear resistance of the soil is kept, the lateral flow and the accompanying settlement are suppressing. Here as well, the approximate model accurately reproduces the predictions of the exact model for the overall deformation in the improved region.

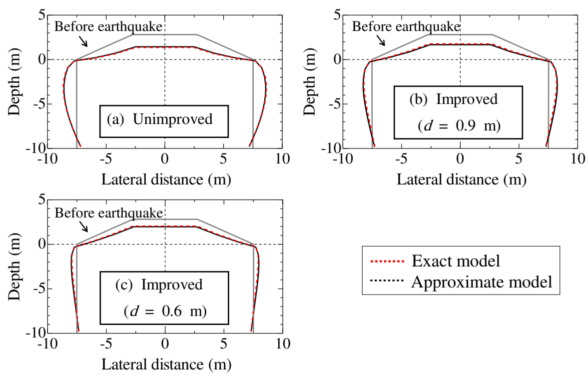

Figure 8. Deformation of improved region and embankment

Figure 9 shows the behaviors of the element at the initial depth of 4.5 m in the center of the improved region. The approximate model provides responses nearly equivalent to those of the exact model in all cases. The two improved cases show that the decrease of the effective stress became smaller during the earthquake as the drain spacing is reduced. Instead, there is greater compression due to compaction during the earthquake. These cases show lower compression due to consolidation after the earthquake, compared to that during the earthquake. Thus, the suppression of increase in pore water pressure and the compaction of the ground that takes place in compensation for this, which are unique features of PWPDM, are accurately reproduced by the calculations of the approximate model.

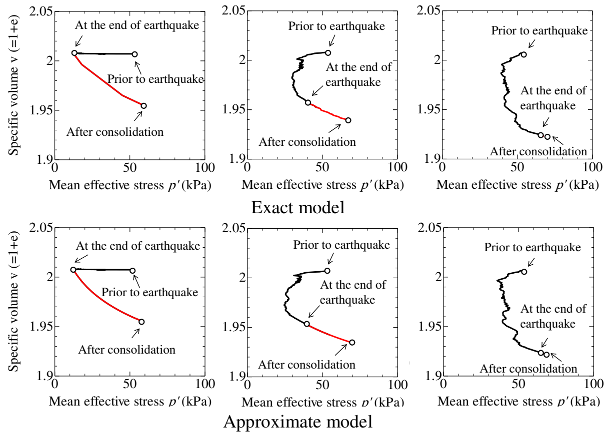

(a) Unimproved (b) Improved (d = 0.9 m) (c) Improved (d = 0.6 m)
Figure 9. Element behavior

Table 4 shows the calculation times during the earthquake in both models. The approximate model required about 1/180 the time needed by the exact model. It is clear that the macro-element method, including the greatly saving labor of dividing mesh, provides a sizeable improvement in calculation efficiency.

Table 4. Calculation time for an earthquake analysis (145sec)

Exact model	1,697,640 sec(19.6 day)
Approximate model	9,630 sec (0.1 day)

4 CONCLUSION

1) The macro-element method expanded by the authors quantitatively approximates the differences in suppression of increase in water pressure due to drain spacing while using a single mesh.
2) The extremely accurate approximation of the effect of suppression in water pressure increase in this method enables accurate quantitative predictions of the effect of suppression in deformation.
3) Application of the macro-element method improves calculation efficiency due to greatly laborsaving in mesh-dividing and dramatically reducing calculation times.

5 ACKNOWLEDGEMENTS

The authors deeply appreciate Prof. Toshihiro Noda of Nagoya University for his support in the present study. This study was also supported by JSPS KEKENHI Grant Number JP25249064.

6 REFERENCES

Noda T., Asaoka A. and Nakano M. 2008. Soil-water coupled finite deformation analysis based on a rate-type equation of motion incorporating the SYS Cam-clay model, *Soils Found.* 45(6), 771-790.

Noda T., Yamada S., Nonaka T. and Tashiro M. 2015. Study on the pore water pressure dissipation method as a liquefaction countermeasure using soil-water coupled finite deformation analysis equipped with a macro element method, *Soils Found.* 55(5), 1130-1139.

Research Association for DEPP Method 2011. *Technical data on dissipation of excess pore water pressure method* (in Japanese).

Sekiguchi H., Shibata T., Fujimoto A. and Yamaguchi H. 1986. A macro-element approach to analyzing the plane strain behavior of soft foundation with vertical drains, *Proc. of the 31st symposium of the JGS, 111-116* (in Japanese).

Yamada S., Noda T., Tashiro M., and Nguyen S. H. 2015. Macro element method with water absorption and discharge functions for vertical drains, *Soils Found.* 55(5), 1114-1129.